NASA Technical Memorandum 84504

NASA-TM-84504 19820022691

THE ROLE OF PEEL STRESSES IN CYCLIC DEBONDING

Richard A. Everett, Jr.

June 1982

National Aeronautics and Space Administration

Langley Research Center
Hampton, Virginia 23665

THE ROLE OF PEEL STRESSES IN CYCLIC DEBONDING

Richard A. Everett, Jr.
Structures Laboratory
U.S. Army Research and Technology Laboratories (AVRADCOM)
NASA Langley Research Center
Hampton, Virginia 23665

If the advantages of adhesively bonded joints, as compared to mechanically fastened joints, are to be exploited, a better understanding of these structural joints in a fatigue load environment is needed. One of the first tasks in an effective study of the fatigue of any structure is to define the possible modes of damage propagation. In metal structures with mechanical fasteners, the growth of a crack from a fastener hole is the principal mode of damage. In adhesively bonded structures there are two potential damage modes--cracking of one of the adherends or cracking of the adhesive. Niranjar (1), in a comprehensive review of bonded joint studies, states that the failure location in metallic lap joints is a function of the cyclic stress level. High cyclic stresses produce failure in the adhesive, whereas low cyclic stresses produce failure in the adherends. In advanced composites Hart-Smith (2) points out that peel-stress-induced fatigue failure will occur in either the adhesive or one of the adherends, depending on whether the peel strength of the adhesive is less than, or greater than, the interlaminar tensile strength of the composite laminate.

When an adhesively bonded joint is undergoing cyclic loading, one of the possible damage modes that can occur, as noted by Blichfeldt and McCarty (3), is called cyclic debonding--progressive separation of the adherends by failure of the adhesive bond under cycling loads. Several basic concepts from fracture mechanics have proven very successful in modeling cyclic debonding. In the

work done by Roderick et al. (4), the concept of strain energy was used to model the cyclic failure of the adhesive bond. In a further refinement of the strain-energy concept, Brussat et al. (5) showed that a more detailed analysis defined the total strain energy associated with the failure of an adhesive bond in terms of the three fracture modes defined in fracture mechanics.

Several papers (Smith and Patterson (6), Ishai and Girshengorn (7), and Hart-Smith (2)) have shown that mode I fracture of the adhesive, where the failure stresses are from tensile loading normal to the bondline, could be the major contributor to the initiation and propagation of cyclic debonding. If these stresses, called peel stresses, do play a significant role, their exact nature must be better understood before efficient adhesively bonded joints can be designed.

The objective of this work is to determine the role of peel stresses on cyclic debonding by a combined experimental and analytical study. Experimentally, this was done by altering the forces that create the peel stresses by applying a clamping force to oppose the peel stresses. The effect of different values of clamping force on the cyclic debond rate was noted to find the clamping force that was just sufficient to stop debond growth or significantly retard the debond growth rate. Then a finite-element analysis was developed to assess the effect of the clamping force on the strain-energy-release rates due to shear and peel stresses. Finally, the analytical and experimental results were compared to show the role of peel stresses on cyclic debonding.

Test Procedures

For this study, the cracked-lap-shear specimen shown in Figure 1 was chosen. A 14-ply laminate of unidirectional graphite/epoxy, T300/5208*, was

adhesively bonded to a 3.18-mm-thick sheet of 2024-T3 aluminum alloy. A room-temperature-curing adhesive, Hysol EA-934*, bonded the adherends. It should be noted that in aircraft structures where adhesives are used to transfer loads between adherends, McCarty et al. (8) have pointed out that elevated-temperature-curing adhesives are used instead of room-temperature adhesives because of their higher strengths. In the present study, because of the differences in thermal expansion between aluminum and unidirectional graphite/epoxy, a room-temperature-curing adhesive was used for bonding to avoid the complex residual thermal stress state caused by an elevated-temperature cure cycle.

In order to monitor the debonding of the adherends, a sheet of photoelastic plastic was bonded to the graphite/epoxy (4). Under load, isochromatic fringes developed in the photoelastic plastic at the debond front as a result of the high strain gradient due to the load transfer between the two adherends. The isochromatics were viewed through a polarizer and quarter-wave plate. The test specimens were photographed at predetermined intervals throughout each test to record the position of the debond front. Debond growth was recorded over 12 cm of the test specimen.

Tests were run in a 100 kN closed-loop servohydraulic test stand at a frequency of 9 Hz. Constant-amplitude cyclic loads were applied at a stress ratio of 0.1, where the stress ratio is defined as the ratio of the minimum to maximum stress in the load cycle. The maximum applied load was 24,464 N, which resulted in a nominal stress of 52 MPa in the unbonded portion of the aluminum.

The peel stresses developed in the adhesive during cyclic debonding were altered experimentally by applying a normal force to the surface of the specimen

*The use of trade names in this article does not constitute endorsement, either expressed or implied, by the National Aeronautics and Space Administration.

through a spring-loaded clamp as shown in Figure 2. A load-deflection curve was developed for the spring-loaded clamp by using small load cells (9). To apply a known normal force to the specimen, the springs were deflected to the appropriate value on the spring's experimentally determined load-deflection curve. The clamping force was accurate within ±45 N.

Experimental Results

Before testing with the clamping force, the cyclic debond behavior of the specimen was characterized during three tests with no alternation of the peel stresses, i.e., no clamp. The results of these tests are shown in Figure 3. The data in Figure 3 indicate an approximately linear relationship between the debond length and the applied load cycles. The slopes of the straight lines faired through the data are defined as the debond propagation rates (4). The debond propagation rates for these tests, from linear regression, varied from 1.37×10^{-4} to 4.47×10^{-4} mm/cycle. The variation in the debond propagation rates between these three specimens for the same applied load is indicative of the scatter in the data from specimen to specimen. Brussat et al. (5) recorded variations of a factor of four in debond rates for their work with the cracked-lap-shear specimen.

To reduce the peel stresses, a clamp force was applied to the specimen about 6 cm beyond the point where the debond initiated. Tests were run at six different values of clamp force to evaluate the effects of the force level on the debond growth rate as the debond front approached and passed the clamp location. Replicate tests were run at most clamp force levels to assure that data scatter would not cause misinterpretation of the results. Clamp force levels and debond rates are listed in Table I. The failure mode in all of these tests was cohesive.

Figure 4 shows a typical variation of debond length with applied load cycles when the clamp was used. Comparison of the initial debond rate in Figure 4 with the test results in Table I for the specimens without any clamping force indicates that the clamp force had no effect on debond rate until the debond front reached the clamp. After the debond front passed under the clamp, however, the debond growth was significantly retarded. The degree of growth retardation was quantified by noting the number of load cycles required to grow the debond 0.5 cm beyond the clamp location. This growth period, called the cyclic retardation period, is listed in Table I for all of the tests. The debond rates after the clamp was removed, Figure 4, were about the same as those measured before the debond front reached the clamp location. This indicates that no residual effect was experienced by the adhesive due to the presence of the clamp.

The effect of the clamp force on the cyclic retardation period is shown in Figure 5. These data show that clamp forces above about 500 N caused dramatically longer retardation periods--essentially stopping the debond growth. Hence, at clamp forces above 500 N, the stresses that are causing the debond to grow have been lowered below a threshold value. To determine the state of the stresses in the adhesive at this condition, a finite-element analysis of the test specimen configuration was conducted.

Analytical Results and Discussion

The forces that define the peel stresses in the adhesive bond are those that are normal to the plane of the debond. These are also the forces that define the mode I fracture parameter, G_I, where G is called the strain-energy-release rate. Strain-energy-release rate is defined as the strain energy

release per unit of new crack area generated (10). It can be thought of as the energy required to extend an existing crack or debond. Since the cracked-lap-shear specimen was developed as a mixed-mode fracture specimen (5), it contains a significant amount of the shear component of the strain-energy-release rate, namely G_{II}, as well as G_I. (For the test specimen configuration used in this study, the finite-element analysis shows that G_{II} is twice G_I.)

Because G_I is the strain-energy-release rate produced by the peel stresses, any change in G_I which occurred during cyclic debonding would reflect a comparable change in the peel stresses in the adhesive bond. Since it has been shown that the strain-energy-release rate correlates cyclic debond rates better than the stresses in the adhesive bond (11), the effects of the clamp force on G_I were used as an indication of the role that peel stresses play in causing cyclic debonding.

To determine the effect of clamping force on the strain-energy-release rate, a finite-element analysis was conducted on the cracked-lap-shear specimen. The finite-element analysis used in this study is a geometrically nonlinear two-dimensional analysis (12). For this analysis, the cracked-lap-shear specimen was simulated by a finite-element model which consisted of 1800 degrees of freedom. A sketch of the model, along with the accompanying boundary conditions and simulated clamp force, are shown in Figure 6. The boundary conditions and degrees of freedom used in this model were chosen based on a convergence study (12) which was designed to simulate the test specimen as it was loaded in the test stand. Friction forces were not included in this analysis. The material properties used in the analysis are given in Table II. To simulate the cohesive failure mode that occurred during debonding, the adhesive was modeled with two elements through the thickness. The clamp force used for this analysis

was 534 N. This was the minimum value of the clamp force used in the tests that essentially stopped cyclic debonding. Several analyses were run varying the relative position of the debond to the clamp force. The results of these analyses are shown in Figure 7. The three curves shown in this figure represent the strain-energy-release rate due to the peel stresses, G_I, the shear stresses, G_{II}, and the total strain-energy-release rate, G_T, which is the sum of G_I and G_{II}. Each point on the curves shows the strain-energy-release rate at the position of the debond front with the clamp force 6 cm beyond where the debond initiated. The strain-energy-release rates shown in Figure 7 where the data are constant show G_T to be 255 J/m^2, G_I is 84 J/m^2, and G_{II} is 171 J/m^2. This constant portion of the curve verifies the experimental results which also showed that the clamp force has no effect on the debond growth until the debond front is a few millimeters from the clamp.

In order to verify the accuracy of the finite-element analysis, an experimental method, which uses the change in the compliance of the test specimen as the debond grows, was used to determine the total strain-energy-release rate of the specimen (12). This method uses an expression developed by Irwin (13),

$$G = \frac{P^2}{2B} \frac{\partial c}{\partial a}$$

where P is the applied load on the specimen, B is the thickness of the specimen, c is the specimen compliance, and a is the debond length. Using this experimental method on the cracked-lap-shear specimen tested in this work, a value of G of 275 J/m^2 was determined at the maximum load in the fatigue cycle (9). As stated previously, this is the total strain-energy-release rate. Currently, there are no experimental methods that can determine G_I and G_{II}

independently of each other in a mixed-mode specimen. It should be noted that the experimental value of G_T is within 8 percent of the value determined by the finite-element analysis. This indicates that the finite-element analysis has simulated the test results with reasonable accuracy.

The results of the finite-element analysis shown in Figure 7 show that the strain-energy-release rate is constant until the debond is about 2 mm ahead of the clamp force. They also show that the shear-strain-energy-release rate, G_{II}, is twice the peel strain-energy-release rate, G_I. As the debond comes within 2 mm of the clamp force, the data in Figure 7 indicate that G_I decreases significantly while G_{II} increases. As stated previously, the debond appeared to grow about 5 mm beyond the clamp before it essentially stopped. The results of the analysis given in Figure 7 show that G_I is about 41 J/m^2 when the debond is under the clamp and decreases to almost zero when the debond is 5 mm past the clamp. Over this 5 mm length, G_{II} increases by about 30 percent. Since the debond rate was much lower after the debond front reached the clamp location, this indicates that it is the strain-energy-release rate, G_I, produced by the peel stresses, that is the principal controlling stress of cyclic debonding.

Since the tests run in this study were at only one value of applied load on the test specimen, only one value of G_T and one ratio of G_I to G_{II} was investigated. Tests with different ratios of G_I to G_{II} need to be conducted to obtain a more complete understanding of the contributions of G_I and G_{II} to the debonding process.

Summary

The role of the peel stresses during cyclic debonding was determined by applying a clamping force to a cracked-lap-shear specimen during a series of constant-amplitude fatigue tests in order to reduce the peel stresses that occur in the adhesive bondline. Tests were conducted over a range of clamping forces to determine the clamping force that just stopped the debond growth. For a maximum applied cyclic load of 24 kN, a clamping force of about 0.5 kN essentially stopped the debond growth.

The effect of the clamping force on the peel stresses was assessed by conducting a finite-element analysis to determine the change in the strain-energy-release rates. Since the mode I strain-energy-rate is generated from the normal forces in the adhesive, any change in G_I indicates a corresponding change in the peel stresses. The analysis showed that a clamping force of 0.5 kN reduced G_I almost to zero, whereas G_{II} increased. These results imply that the peel stress that generates G_I is the principal stress causing cyclic debonding. However, additional tests with different G_I to G_{II} ratios and tests on other adhesives should be conducted before it can be concluded that the peel stresses are the principal cause of cyclic debonding in all joint configurations.

References

1. Niranjar, V.: Bonded Joints--A Review for Engineers. UTIAS Review No. 28, University of Toronto Institute for Aerospace Studies, 1970.

2. Hart-Smith, L. J.: Analysis and Design of Advanced Composite Bonded Joints. NASA CR-2218, 1973.

3. Blichfeldt, B.; and McCarty, J. E.: Analytical and Experimental Investigation of Aircraft Metal Structures Reinforced with Filamentary Composites. NASA CR-2039, 1972.

4. Roderick, G. L.; Everett, R. A., Jr.; and Crews, J. H., Jr.: Debond Propagation in Composite-Reinforced Metals. Fatigue of Composite Materials, ASTM STP 569, American Society for Testing and Materials, 1975, pp. 295-306.

5. Brussat, T. R.; Chiu, S. T.; and Mostovoy, S.: Fracture Mechanics for Structural Adhesive Bonds. AFML-TR-77-163, Air Force Materials Laboratory, 1977.

6. Smith, C. S.; and Patterson, D.: Design of Structural Connections in GRP Ship and Boat Hulls. Designing with Fiber Reinforcing Materials, Institute of Mechanical Engineers Conference Publications 1977-79, 1977.

7. Ishai, O.; and Girshengorn, T.: Strength of Bonded Aluminum-CFRP Single-Lap Joints. Adhesives Age, July 1978.

8. McCarty, J. E.; Horton, R. E.; and Locke, M. C.: Repair of Bonded Primary Structure. AFFDL-TR-78-79, Air Force Flight Dynamics Laboratory, 1978.

9. Everett, R. A., Jr.: The Significance of Peel Stresses in Cyclic Debonding. M.S. Thesis, Old Dominion University, 1980.

10. Paris, P. C.; and Sih, G. C.: Stress Analysis of Cracks. Fracture Toughness Testing and Its Applications, ASTM STP 381, American Society for Testing and Materials, 1965, pp. 30-81.

11. Roderick, G. L.; Everett, R. A., Jr.; and Crews, J. H., Jr.: Cyclic Debonding of Unidirectional Composite Bonded to Aluminum Sheet for Constant Amplitude Loading. NASA TN D-8126, 1976.

12. Dattaguru, B.; Everett, R. A., Jr.; Whitcomb, J. D.; and Johnson, W. S.: Geometrically-Nonlinear Analysis of Adhesively Bonded Joints. Presented at the 23rd AIAA/ASME/ASCE/AHS Structures, Structural Dynamics, and Materials Conference, New Orleans, LA, May 1982.

13. Irwin, G. R.: Fracture Mechanics. Proceedings of the First Symposium on Naval Structural Mechanics, 1958.

TABLE I.- TEST RESULTS

Specimen number	Clamp force, N	Cyclic retardation period, cycles	Debond growth rate before reaching clamp location, x 10^{-4} mm/cycle	Debond growth rate after clamp removed, x 10^{-4} mm/cycle
PU2-1	0		4.5	
PU3-2	0		2.8	
PU5-5	0		1.4	
PU1-4	222	60,000	4.1	...
PU2-2	222	77,250	4.0	1.7
PU2-4	334	67,000	3.1	2.9
PU5-2	334	110,000	3.0	1.1
PU2-3	445	81,000	5.5	...
PU2-5	445	93,000	6.1	4.6
PU4-3	534	5,490,000	6.5	2.6
PU5-1	534	4,125,510	0.9	1.3
PU4-1	623	2,450,000	1.3	1.5
PU4-4	800	3,964,000	1.4	1.8

TABLE II.- MATERIAL PROPERTIES

Material	Axial elastic modulus, GPa	Transverse elastic modulus, GPa	Poisson's ratio	Shear modulus, GPa
Aluminum	71.0	71.0	0.33	26.5
Graphite/Epoxy	131.0	11.7	0.019	4.48
EA-934	4.14	4.14	0.40	1.48

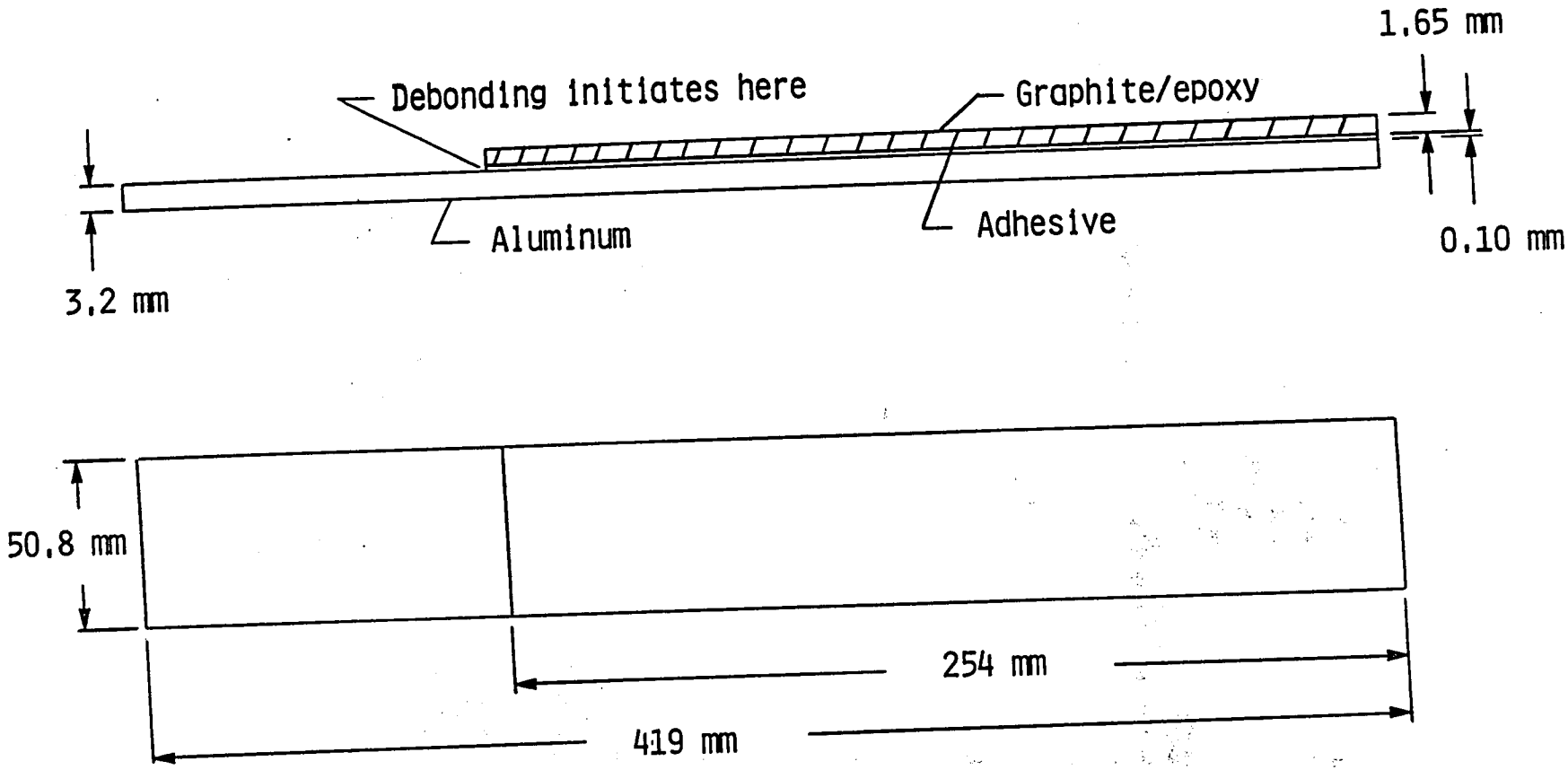

Figure 1.- Cracked-lap-shear specimen.

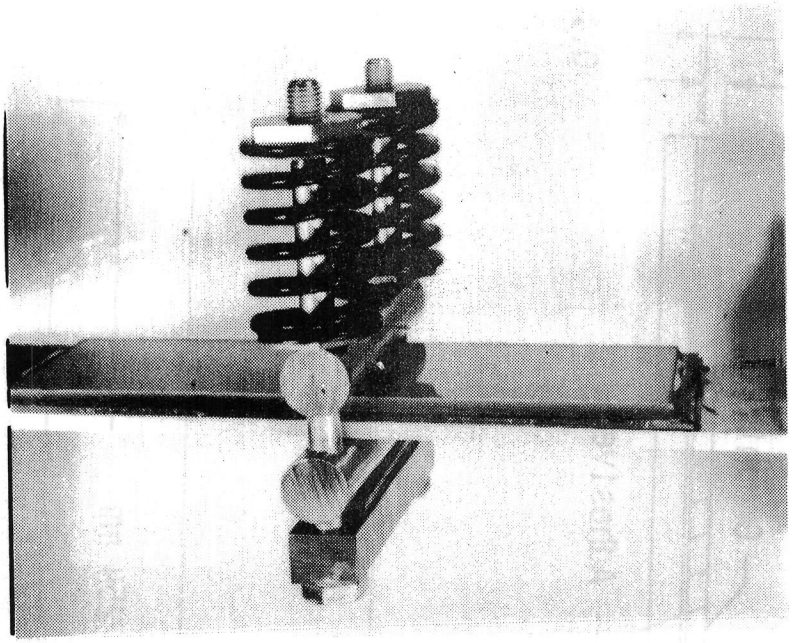

Edge view.

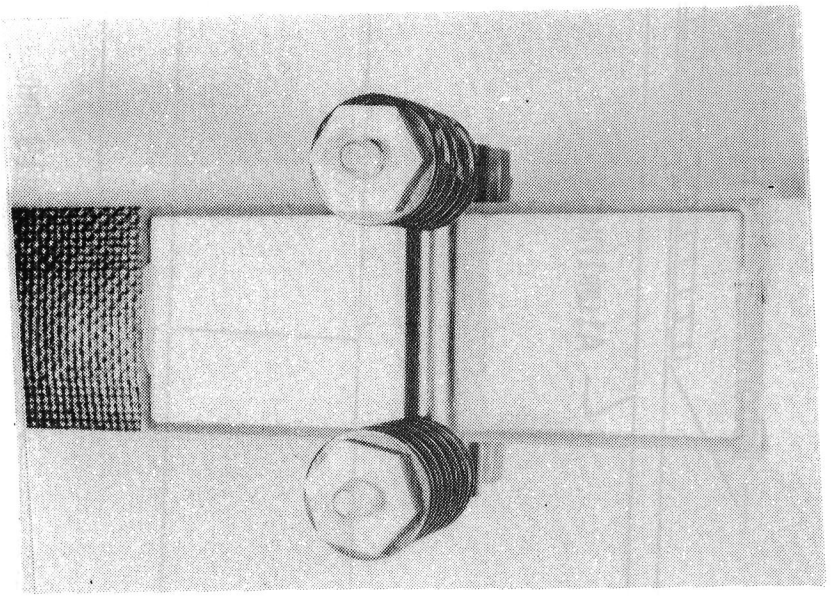

Top view.

Figure 2.- Spring-loaded clamp.

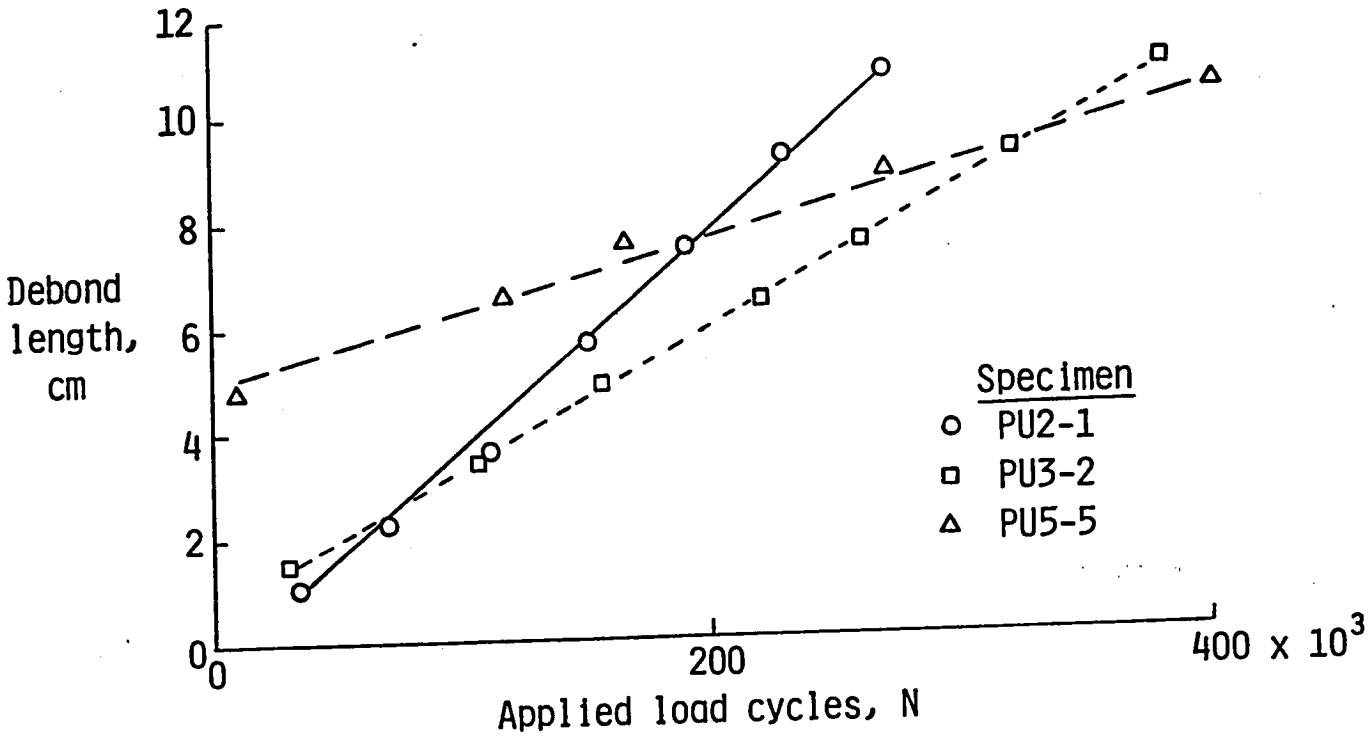

Figure 3.- Typical debonding behavior.

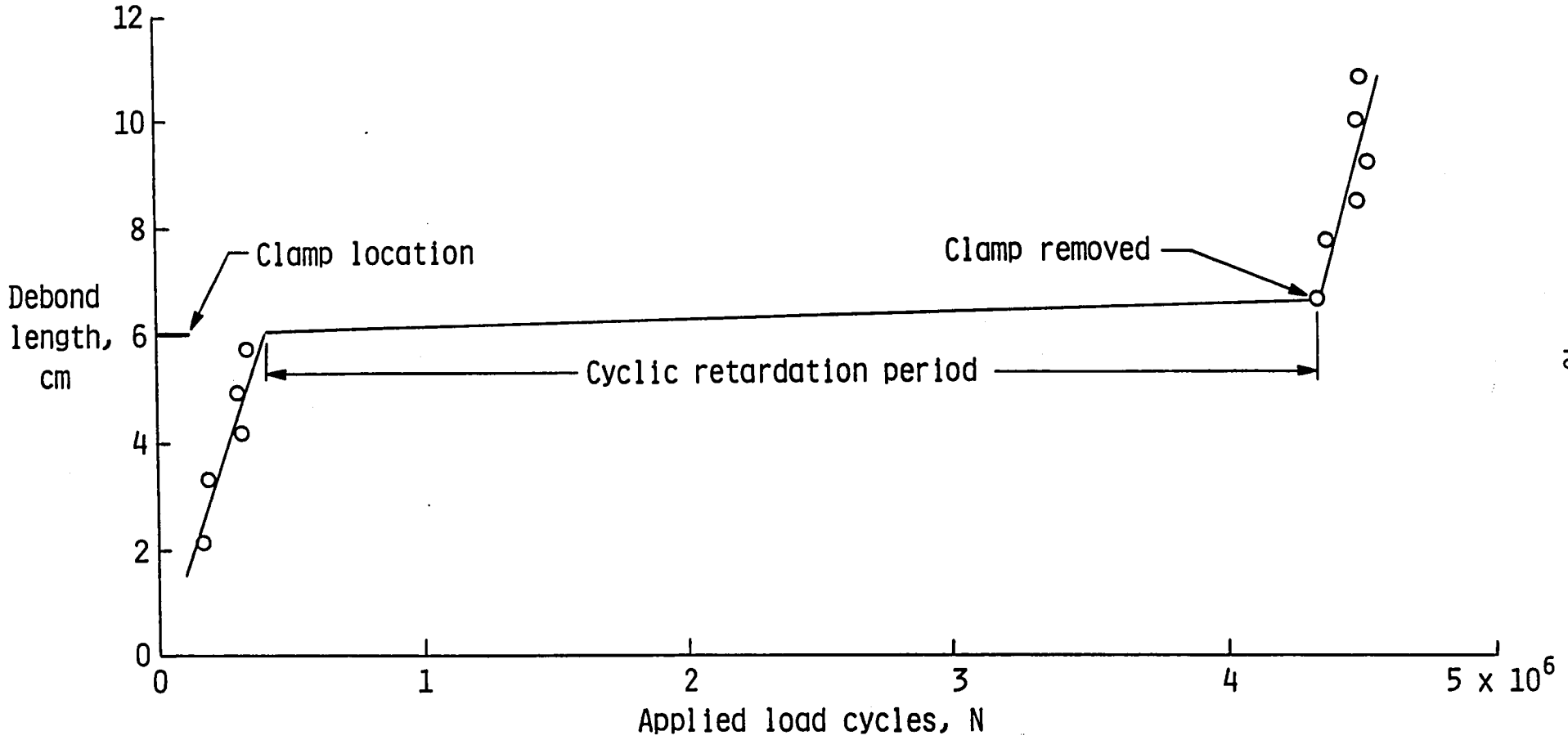

Figure 4.- Debond behavior for a clamp force of 800 N.

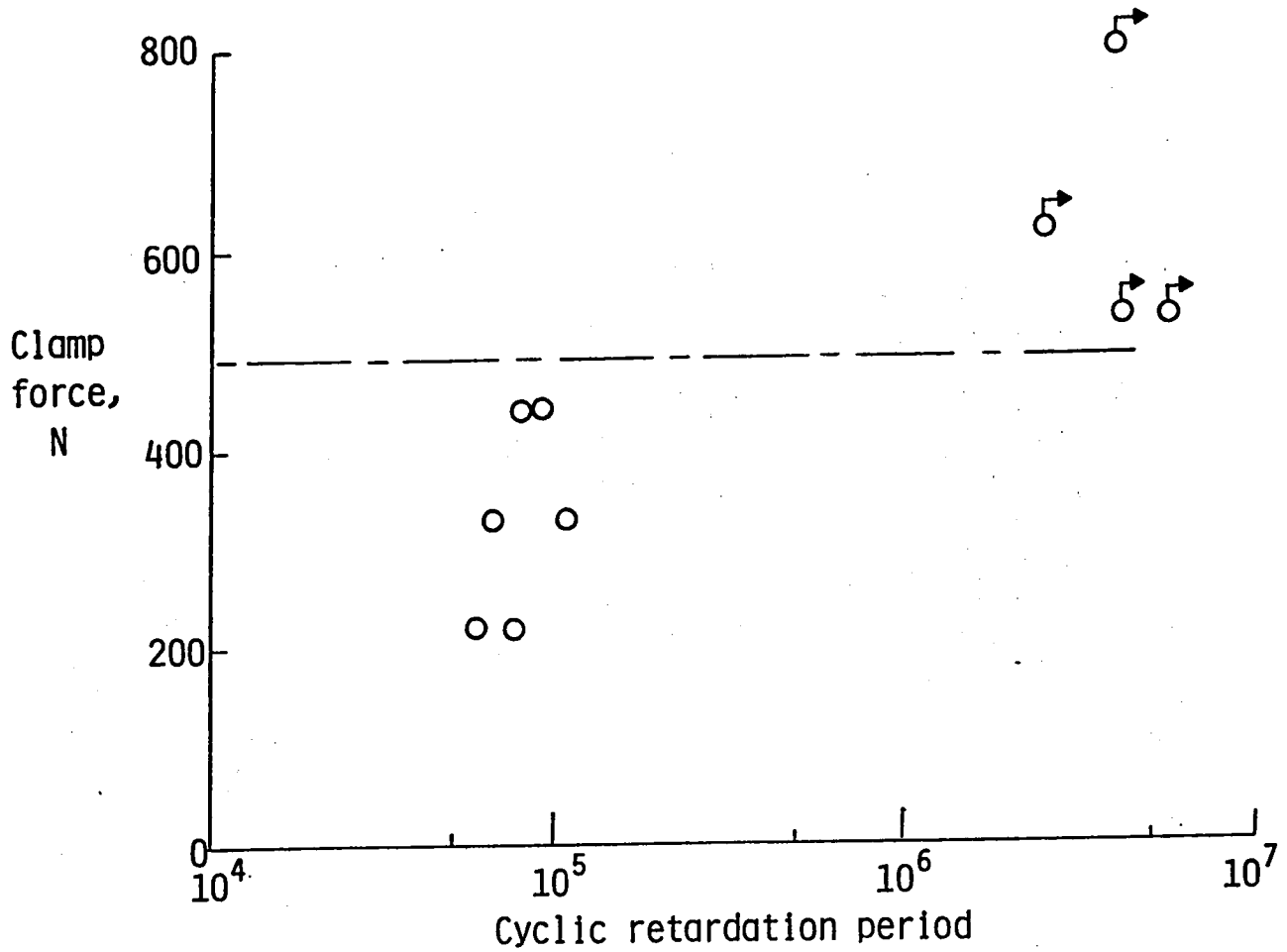

Figure 5.- Clamp force versus cyclic retardation period.

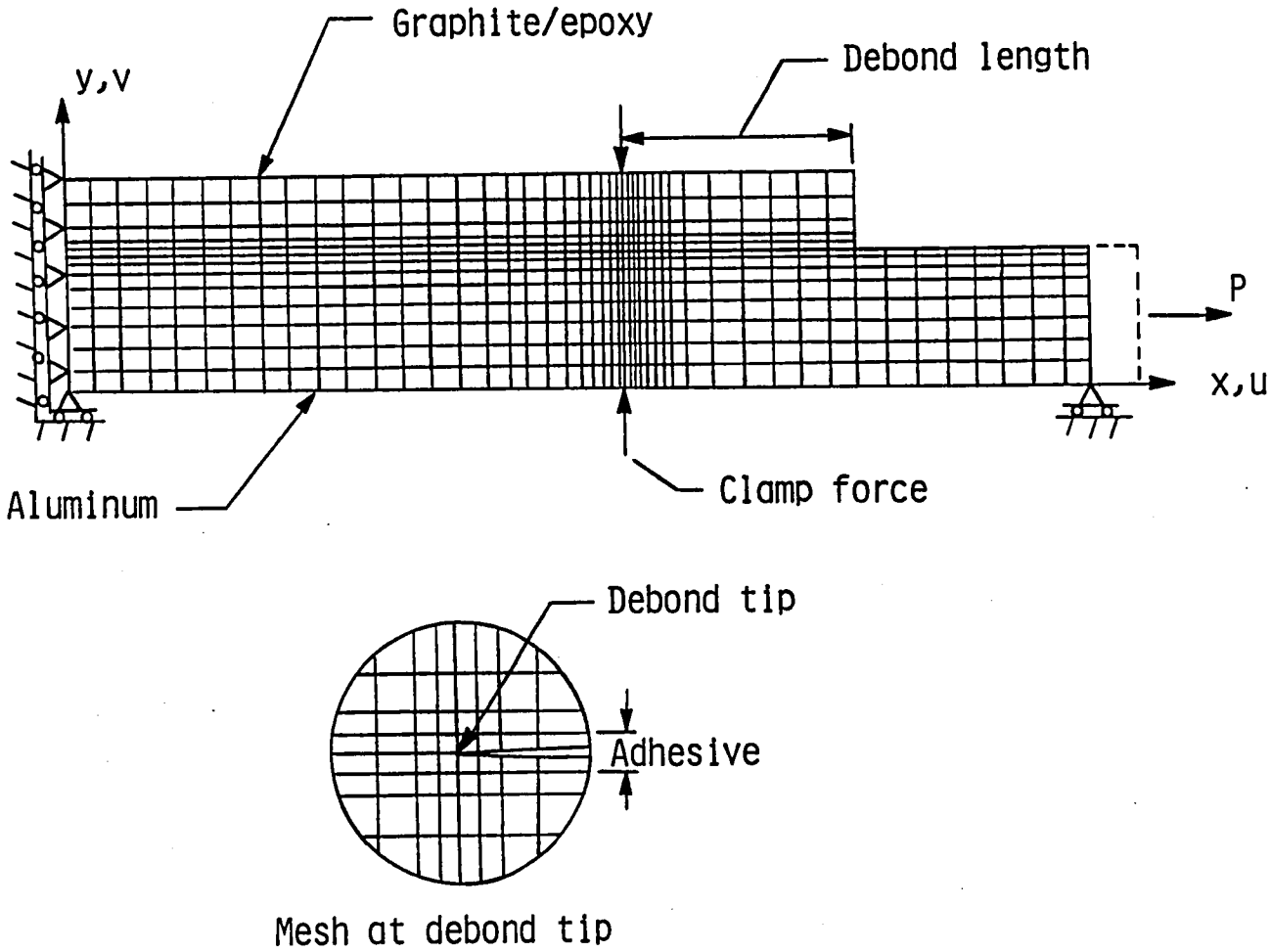

Figure 6.- Finite-element mesh of cracked-lap-shear specimen.

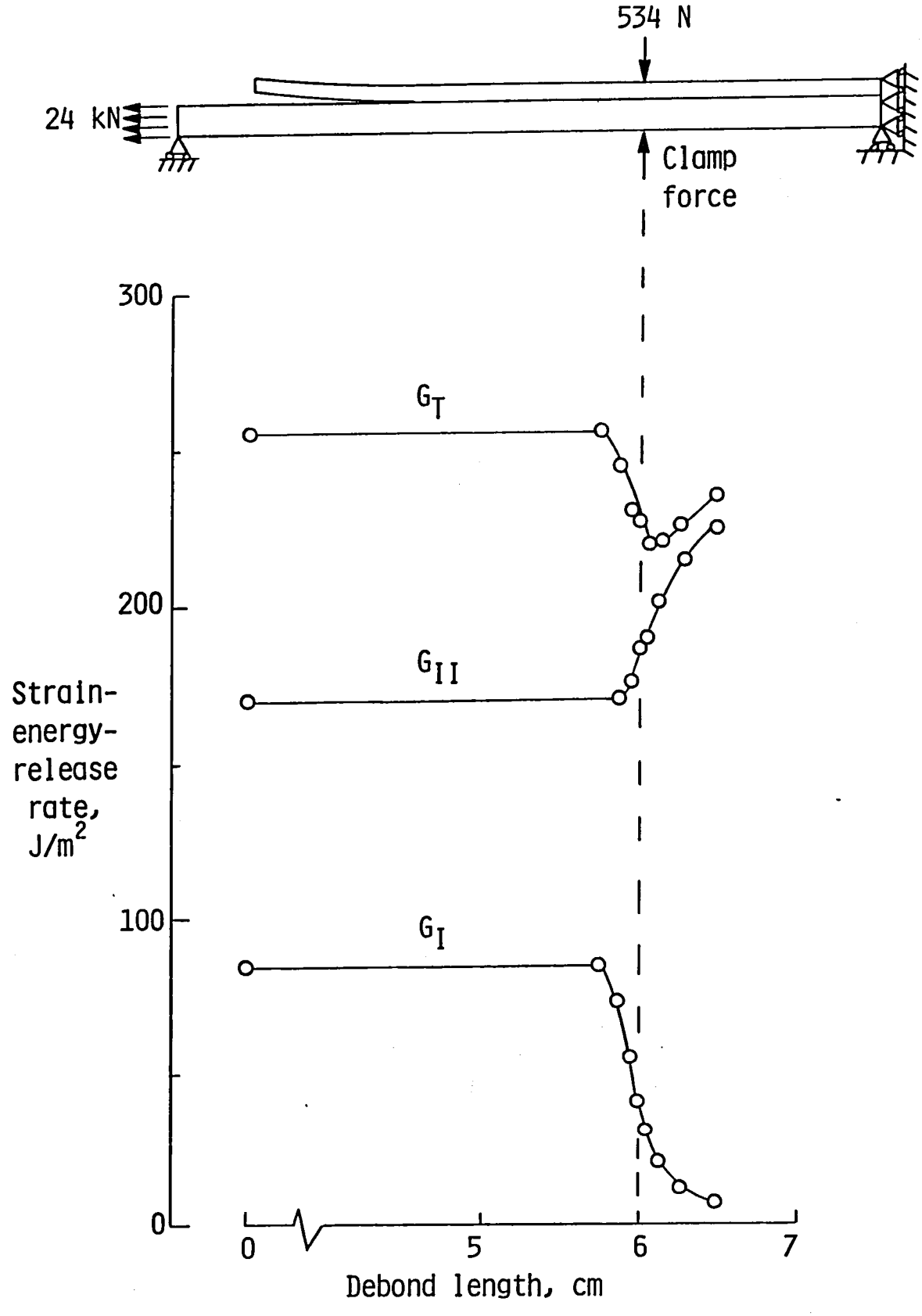

Figure 7.- Finite-element results.

1. Report No.	2. Government Accession No.	3. Recipient's Catalog No.
NASA TM-84504		

4. Title and Subtitle	5. Report Date
THE ROLE OF PEEL STRESSES IN CYCLIC DEBONDING	June 1982
	6. Performing Organization Code 505-33-33-05
7. Author(s) Richard A. Everett, Jr.	8. Performing Organization Report No.
	10. Work Unit No.
9. Performing Organization Name and Address NASA Langley Research Center Hampton, VA 23665	11. Contract or Grant No.
	13. Type of Report and Period Covered Technical Memorandum
12. Sponsoring Agency Name and Address National Aeronautics and Space Administration Washington, DC 20546	14. Sponsoring Agency Code

15. Supplementary Notes

16. Abstract

When an adhesively bonded joint is undergoing cyclic loading, one of the possible damage modes that occurs is called cyclic debonding--progressive separation of the adherends by failure of the adhesive bond under cyclic loading. In most practical structures, both peel and shear stresses exist in the adhesive bondline during cyclic loading. This paper presents the results of an experimental and analytical study to determine the role of peel stresses on cyclic debonding in a mixed-mode specimen. Experimentally, this was done by controlling the forces that create the peel stresses by applying a clamping force to oppose the peel stresses. Cracked-lap-shear joints were chosen for this study. A finite-element analysis was developed to assess the effect of the clamping force on the strain-energy-release rates due to shear and peel stresses. The results imply that the peel stress is the principal stress causing cyclic debonding.

17. Key Words (Suggested by Author(s))	18. Distribution Statement
Peel stress Fatigue Cyclic debonding Cracked-lap-shear specimen Finite-element analysis	Unclassified - Unlimited Subject Category 39

19. Security Classif. (of this report)	20. Security Classif. (of this page)	21. No. of Pages	22. Price*
Unclassified	Unclassified	20	A02

* For sale by the National Technical Information Service, Springfield, Virginia 22161